第 40 卷　第 3 期
2025 年 6 月

新型炭材料（中英文）
New Carbon Materials

Cite this: New Carbon Materials, 2025, 40(3): 641-649

Read Online

Research article

Microwave-enabled rapid, continuous, and substrate-free synthesis of few-layer graphdiyne nanosheets for enhanced potassium metal battery performance

KONG Ya[1,2,†], ZHANG Shi-peng[3,†], YIN Yu-ling[4,5], ZHANG Zi-xuan[1], FENG Xue-ting[1],
DING Feng[4,6], ZHANG Jin[1], TONG Lian-ming[1,7,*], GAO Xin[1,*]

(1. *School of Materials Science and Engineering*, *Beijing National Laboratory for Molecular Sciences*, *College of Chemistry and Molecular Engineering*, *Peking University*, *Beijing* 100871, *China*;
2. *China Academy of Aerospace System and Innovation*, *Beijing* 100088, *China*;
3. *State Key Laboratory of Solidification Processing*, *Center for Nano Energy Materials*, *School of Materials Science and Engineering*, *Northwestern Polytechnical University and Shanxi Joint Laboratory of Graphene (NPU)*, *Xi'an* 710072, *China*;
4. *Suzhou Laboratory*, *Suzhou* 215123, *China*;
5. *Institute of Technology for Carbon Neutrality*, *Shenzhen Institute of Advanced Technology*, *Chinese Academy of Sciences*, *Shenzhen* 518055, *China*;
6. *Materials Science and Energy Engineering*, *Shenzhen University of Advanced Technology*, *Shenzhen* 518055, *China*;
7. *School of Advanced Materials*, *Peking University Shenzhen Graduate School*, *Shenzhen* 518055, *China*)

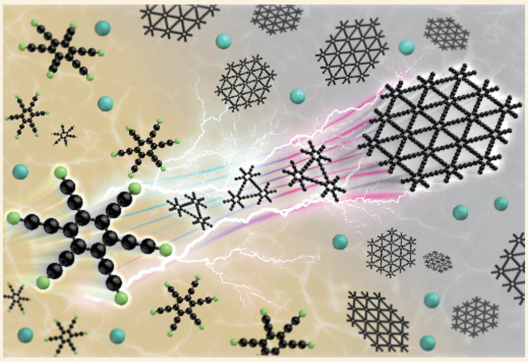

Abstract: Graphdiyne (GDY) is a two-dimensional carbon allotrope with exceptional physical and chemical properties that is gaining increasing attention. However, its efficient and scalable synthesis remains a significant challenge. We present a microwave-assisted approach for its continuous, large-scale production which enables synthesis at a rate of 0.6 g/h, with a yield of up to 90%. The synthesized GDY nanosheets have an average diameter of 246 nm and a thickness of 4 nm. We used GDY as a stable coating for potassium (K) metal anodes (K@GDY), taking advantage of its unique molecular structure to provide favorable paths for K-ion transport. This modification significantly inhibited dendrite formation and improved the cycling stability of K metal batteries. Full-cells with perylene-3,4,9,10-tetracarboxylic dianhydride (PTCDA) cathodes showed the clear superiority of the K@GDY anodes over bare K anodes in terms of performance, stability, and cycle life. The K@GDY maintained a stable voltage plateau and gave an excellent capacity retention after 600 cycles with nearly 100% Coulombic efficiency. This work not only provides a scalable and efficient way for GDY synthesis but also opens new possibilities for its use in energy storage and other advanced technologies.

Key words: Graphdiyne；Microwave-assisted synthesis；Few-layer；Potassium metal battery；Dendrite-free

1 Introduction

Graphdiyne (GDY) is a two-dimensional (2D) carbon allotrope featuring a unique sp/sp^2 hybridized framework, where hexagonal and triangular carbon rings are interconnected by acetylenic linkages[1–2]. The incorporation of sp-hybridized carbon atoms imparts exceptional physical and chemical properties, such as a uniform subnanometer pore structure, a moderate band gap of 0.44 to 1.47 eV[2–9], and a delocalized conjugated electronic structure, making GDY highly suitable for applications in electronics[10–13], catalysis[14–16], energy storage and conversion[17–20], and gas separation[21–23]. Additionally, GDY exhibits remarkable mechanical strength[24] and unique nonlocal infrared response[13,25], positioning it as one of the

Received: February 28, 2025
Revised: April 30, 2025
Accepted: April 30, 2025
DOI: 10.1016/S1872-5805(25)60987-5
CSTR: 32158.14.S1872-5805(25)60987-5

most promising carbon materials for next-generation technologies.

Despite these advantages, scaling up the production of high-quality GDY powders remains challenging. The primary obstacles include: (1) The instability of sp-hybridized carbon atoms, which are prone to oxidation under high-temperature preparation conditions[1,26]. (2) The rotational flexibility of C—C in GDY, makes it difficult to control crystallinity and thickness[27–28]. (3) The inefficiency of deprotection operations involving the monomer hexakis-[(trimethylsilyl)ethynyl]benzene (HEB-TMS)[29]. These limitations render traditional high-temperature chemical vapor deposition (CVD) methods unsuitable for synthesizing GDY on a large scale.

Various techniques have been developed to overcome these challenges, with wet chemistry-based confinement methods being the most common. These approaches, such as using graphene as a substrate to facilitate the in-plane growth of GDY by van der Waals interactions[30], improve crystallinity. However, difficulties in separating GDY from the substrate hinder the isolation of intrinsic GDY[31–32]. Other methods, such as gas/liquid and liquid/liquid interfacial techniques, have also been employed to produce multilayer GDY nanosheets. However, substrate limitations and the inability to control the growth of GDY due to its structural flexibility have restricted large-scale production.

Here, we present a microwave-assisted chemical synthesis method that enables the continuous, large-scale production of GDY without the need for substrates. Using HEB-TMS as the precursor, copper chloride (CuCl) as the catalyst, and N, N-dimethylformamide (DMF) as the solvent, we synthesized GDY at a rate of 0.6 g/h with yields of up to 90%. The synthesized GDY nanosheets, with an average diameter of 246 nm and thickness of 4 nm, were then applied as a stable coating on potassium (K) metal anode. This modification not only provided abundant binding sites for K^+ but also facilitated ionic conductivity, effectively inhibiting the formation of K dendrites and enhancing battery cycling stability. The rapid and continuous synthesis method developed in this study opens new possibilities for applications of GDY in various fields, particularly in energy storage systems.

2 Experimental

2.1 Materials

Trimethylsilylacetylene was purchased from Woerjimimg (Beijing) Technology Development Institute. Ultradry tetrahydrofuran, N-butyllithium and hexabromobenzene were obtained from J&K Scientific. Zinc chloride was purchased from Alfa Aesar. N,N-Dimethylformamide (DMF) and pyridine were supplied by Concord Technology. Tetrakis(triphenylphosphine)-palladium (0) and Copper (I) chloride (CuCl) were obtained from Macklin.

2.2 Synthesis of GDY Nanosheets

The GDY nanosheets were synthesized by an alkynylsilane coupling reaction using microwave-assisted synthesis. First, 25 mg of CuCl was dissolved in 100 mL of DMF and sonicated for 20 min. Then, 300 mg of HEB-TMS was added to the solution and stirred for 5 min to ensure full dissolution. The reaction mixture was subsequently microwave-treated (Model: MCR-3) at 135 °C for 5 min. Finally, the product was washed sequentially with pyridine, acetone, and distilled water. Pure GDY nanosheets were then obtained by freeze-drying.

2.3 Material characterization

Morphological and structural characterization was performed using transmission electron microscopy (FEI Tecnai F20 electron microscope operating at 200 kV) and atomic force microscopy (Bruker Dimension Icon, Scan Asyst) images were obtained with a height sensor. Raman spectra were recorded using a Horiba HR800 Raman system with a laser excitation wavelength of 532 nm and a spot size of approximately 1 μm. X-ray photoelectron spectroscopy measurements were conducted with a Kratos Axis Ultra-DLD spectrophotometer (AXIS Supra, Kratos Analytical Ltd.) using monochromatic Al X-ray under low pressure (5×10^{-9} to 1×10^{-8} mmL/g). X-ray diffraction (XRD) patterns were characterized by Rigaku (Smat-

Lab SE, Japan) in the 2θ range of 10°-90°. The thermogravimetric analysis (TGA) was obtained on a Q600 SDT withunder the atmosphere of nitrogen at a heating rate of 10 K min^{-1}.

3 Results and discussion

2D homogeneous synthesis of GDY presents several challenges, primarily due to the competition between in-plane and out-of-plane growth. From a kinetic perspective, three-dimensional (3D) spherical growth typically occurs faster than 2D in-plane growth. Thermodynamically, staggered structures often reduce repulsion between chemical bonds, favoring out-of-plane growth[33–34]. To better understand the growth process of GDY and guide experimental design, we conducted theoretical calculations on the coupling of hexaethynylbenzene (HEB) monomers (Fig. S1). The energy differences between HEB dimers with rotation angles of 0°, 30°, 60°, and 90° are negligible, suggesting low rotational barriers (Fig. S2). However, the energy of the HEB trimer at 0° rotation angle is significantly lower than that of other rotated configurations, with energy differences of 0.34 eV for a 0°-30° rotation and 0.45 eV for a 90°-90° rotation (Fig. 1a and Fig. 1b). This indicates that the most stable configuration occurs with a 0° rotation. The conjugated triangle of the alkyne and benzene rings locks the structure in-plane, a phenomenon known as the bond-planarity effect. This structure stability is further enhanced by an increase in conjugate enthalpy, leading to a significant extension of delocalization stability across the entire 2D GDY structure.

Building on these insights, we utilized microwave assistance to rapidly increase the temperature of the polar solvent, promoting the coupling reaction and facilitating the fast formation of the first-layer GDY conjugated rings (the HEB trimer). This approach reduces the possibility of rotation between the dimers and accelerates in-plane growth. For the second layer of GDY, the energy difference between the most stable in-plane configuration and the rotated 90° dimer is approximately 1.17 eV (Fig. S3). The energy differences for 30° and 60° rotations are 0.99 and 1.14 eV, respectively. The underlying template enhances the local concentration of HEB monomers, leading to faster in-plane growth. The interlayer van der Waals forces, analogous to those in previously reported graphene templates, promote this in-plane growth under microwave irradiation.

The rapid, continuous, and substrate-free preparation process of GDY nanosheets is depicted in Fig. 1c. The reaction utilizes HEB-TMS as the precursor, CuCl as the catalyst, and DMF as the solvent. Upon microwave irradiation, the polar DMF solvent undergoes rapid molecular vibration, raising the temperature quickly throughout the reaction system. Un-

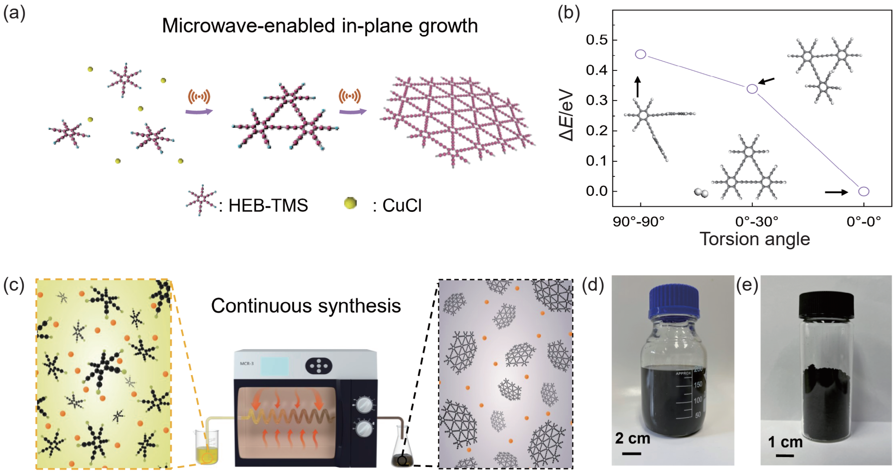

Fig. 1 Microwave-enabled rapid, continuous, and substrate-free synthesis of GDY nanosheets. (a) Schematic diagram of microwave-enabled in-plane growth of GDY. (b) Energy differences of the HEB trimer at various rotation angles: 90°-90°, 0°-30°, and 0°-0°. (c) Microwave-assisted continuous synthesis of GDY. Photographs of (d) 200 mL GDY suspension and (e) GDY powder after freeze-drying

der Cu(I) catalysis, the protective group of HEB-TMS is eliminated, forming an intermediate[35]. Reductive elimination reactions then occur, producing 1,3-butadiyne species, which facilitate the rapid generation of GDY trimers that lock the structure in-plane. A mixed solution of monomers and catalysts is introduced at one end of the pipe, and GDY powder is collected at the opposite end under continuous microwave irradiation. This design enables the rapid, continuous, and substrate-free synthesis of GDY, with a yield exceeding 90% and a production rate of 0.6 g/h under optimized conditions. The resulting suspension (Fig. 1d) is subjected to washing and freeze-drying to produce GDY powder, as illustrated in Fig. 1e.

The morphology and composition of the synthesized powder were characterized using transmission electron microscopy (TEM), atomic force microscopy (AFM), and X-ray photoelectron spectroscopy (XPS). The TEM image (Fig. 2a) reveals uniform nanosheet-like structures of the as-prepared GDY. The AFM image (insert in Fig. 2a) shows a flat surface, confirming the few-layer nature of the GDY nanosheets with a typical thickness of 4 nm. High-resolution TEM (HRTEM) image (Fig. 2b) displays lattice fringes with a spacing of 0.47 nm, which aligns with theoretical predictions[30], indicating well-ordered crystal structures in the GDY nanosheets. The statistical data of lateral sizes extracted from 70 independent domains show a narrow distribution centered around 246 nm, with a range from 185 to 315 nm (Fig. 2c).

Fig. 2d reveals that the GDY nanosheets are primarily composed of carbon (C), aligning well with the energy-dispersive spectroscopy (EDS) mapping results (Fig. S4). The high-resolution C 1s XPS spectrum (Fig. 2e) exhibits three subpeaks at 284.5, 285.2 and 287.0 eV, corresponding to C−C(sp^2), C—C(sp) and C−O bonds, respectively. The area ratio of sp and sp^2 hybridized carbon is approximately 2:1, consistent with the theoretical expectations for GDY. The small amounts of C−O species may be attributed to trace impurities or defects in the sample. Raman spectroscopy (Fig. 2f) further characterizes the structural properties of GDY, with the peak at 2172 cm^{-1} corres-

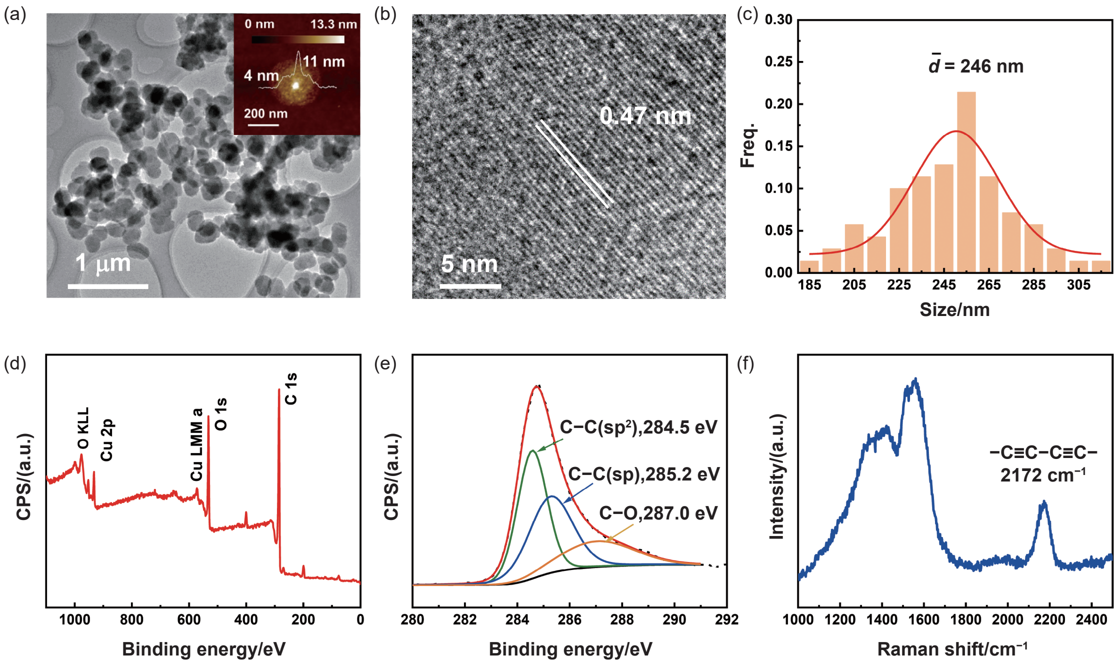

Fig. 2 Characterization of GDY nanosheets. (a) TEM image of the as-prepared GDY nanosheets. Insert: AFM image of the GDY nanosheets. (b) HRTEM image of GDY nanosheets. (c) Size distribution of the GDY nanosheets, with diameters ranging from 185 to 315 nm, averaging 246 nm. (d) Full XPS spectrum of GDY nanosheets. (e) High-resolution C 1s XPS spectrum of GDY nanosheets, with peaks corresponding to C−C(sp^2), C—C(sp) and C−O bonds (dotted line: raw data, solid lines: fitting curves). (f) Raman spectrum of GDY nanosheets, featuring peaks at 2172 cm^{-1} (−C≡C−C≡C−), indicating the characteristic structure of GDY

ponding to the C≡C in 1,3-butadiyne, confirming successful GDY synthesis. The *D* and *G* bands at 1419 and 1553 cm^{-1}, respectively, are attributed to the aromatic rings. XRD (Fig. S5) and TGA (Fig. S6) were also performed to verify the crystallinity and the thermal stability of GDY. Additionally, the specific surface area of the GDY nanosheets is measured to be 362.9 $m^2 \cdot g^{-1}$ (Fig. S7). All these results demonstrate that high-quality, few-layer GDY nanosheets were successfully synthesized by an efficient, microwave-enabled, rapid, continuous and substrate-free method.

The unique molecular structure of GDY offers abundant sites for K binding, both adjacent to the butadiyne within the subnanometer micropores and at the center of the benzene rings. This microporous structure also facilitates ion transport by forming ion tunnels, allowing for efficient K^+ movement. The combination of high K affinity, ionically conductive channels and high surface area makes GDY an ideal candidate for use as an interfacial protection layer in K metal batteries.

As a demonstration, here, GDY nanosheets were applied as a stable coating for K metal anodes, taking advantage of their unique structure to create favorable pathways for K^+ transport. The GDY protection layer was directly painted onto the K metal surface, forming the K@GDY configuration. Symmetric cells using both K@GDY and bare K foil as electrodes were assembled in CR2032 coin cells to explore the K stripping/plating process. A carbonated electrolyte, consisting of 1 mol L^{-1} potassium bis (fluorosulfonyl) imide (KFSI) salts dissolved in a 1∶1 (*v*/*v*) mixture of ethylene carbonate (EC) and diethyl carbonate (DEC), was employed. This electrolyte composition is commonly used in potassium-based systems, known for its stability and ability to support efficient ion transport during the cycling of K metal batteries.

The long-term stability of K plating/stripping was assessed through galvanostatic cycling. The cycling performance and plating/stripping profiles of K@GDY cells were compared to those of bare K cells at a current density of 0.5 $mA \cdot cm^{-2}$ and a capacity rate of 0.5 $mAh \cdot cm^{-2}$ (Fig. 3a). The K@GDY electrode exhibited superior, stable plating/stripping behavior for over 677 h, with a low polarization voltage of approximately 200 mV (Fig. 3b). In contrast, the symmetric cells with bare K electrodes displayed a larger polarization voltage of approximately 350 mV, showing a significant voltage drop after 150 h due to the short-circuit. To further evaluate the effectiveness of the GDY coating, we compared its performance with other carbon materials, such as graphene (Gr). The K@Gr symmetric cells showed a higher polarization voltage of approximately 320 mV after 190 h of cycling (Fig. S9), confirming the superior inhibiting effect and electrochemical performance of the GDY coating. Furthermore, at current densities ranging from 0.5 to 8 $mA \cdot cm^{-2}$ (Fig. 3c), the K@GDY electrode exhibited a voltage hysteresis consistently below 210 mV, indicating superior stability in polarization voltage relative to bare K electrodes. The K@GDY electrode exhibited lower polarization voltage and maintained stability upon returning to 0.5 $mA \cdot cm^{-2}$, whereas symmetric cells with bare K electrodes showed a short-circuit.

The effectiveness of the GDY interfacial layer was further demonstrated by evaluating the morphology of K stripping/plating. In symmetric cells with bare K foil, nonuniform K nucleation and deposition led to the formation of potassium dendrites (Fig. 3d). After 100 cycles of galvanostatic stripping and plating at 0.5 $mA \cdot cm^{-2}$, K dendrites and inactive K (dead K) were clearly visible (Fig. 3e). However, the K metal with the GDY coating effectively eliminated current gathering at the dendrite tips, suppressing dendritic growth (Fig. 3f, g). These results highlight the effectiveness of GDY nanosheets as a protective interfacial layer that significantly enhances the cycling stability and safety of K metal batteries by suppressing dendritic growth and minimizing polarization.

To further showcase the superior performance of the K@GDY anode, we constructed full cells using perylene-3,4,9,10-tetracarboxylic dianhydride (PTCDA) as cathodes (Fig. 4a). The full cell tests with PTCDA cathodes clearly demonstrate the significant advantages of K@GDY anodes over bare K an-

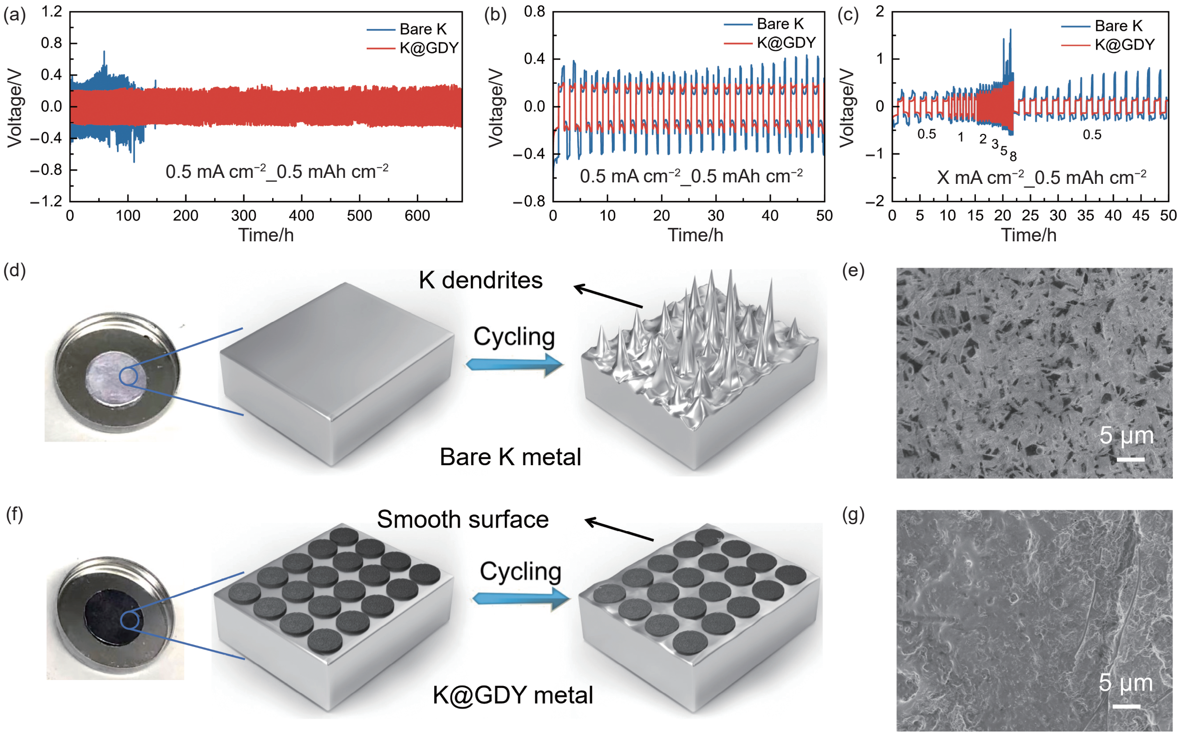

Fig. 3 Symmetric cell cycling performance for K@GDY and K foil electrodes. (a,b) Cycling performance and plating/stripping profiles of symmetrical K@GDY and bare K batteries at 0.5 mA·cm^{-2} and 0.5 mAh·cm^{-2}. (c) Rate performance of the bare K and K@GDY with a fixed capacity of 0.5 mAh·cm^{-2} at various rates of 0.5-8 mA·cm^{-2}. (d) Schematic illustration of K plating/stripping behavior on bare K. (e) SEM image (top-down view) of K deposited on bare K. (f) Schematic illustration of K plating/stripping behavior on K@GDY. (g) SEM image (top-down view) of K deposited on K@GDY

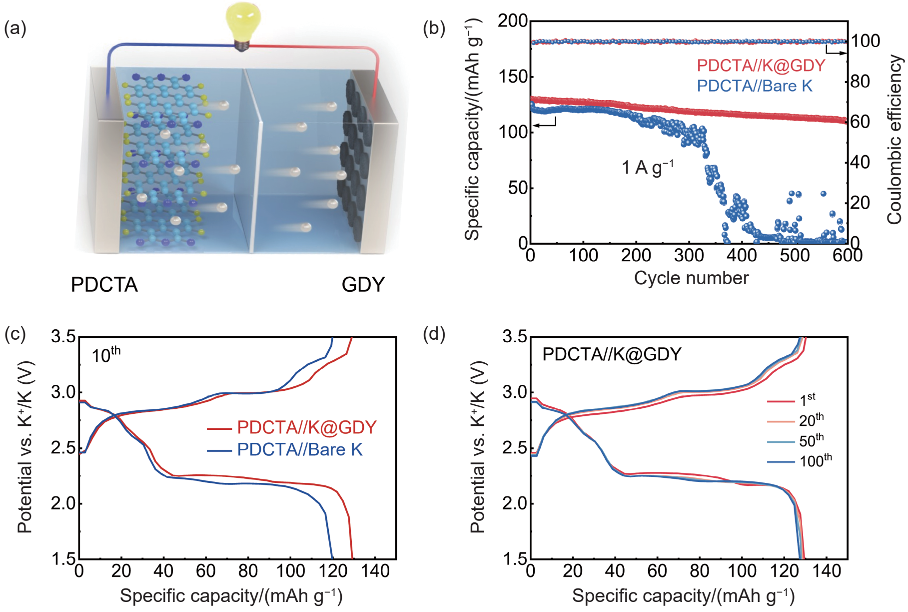

Fig. 4 Full cell cycling performance. (a) Schematic illustration of the PDCTA//K@GDY full cell. (b) The long cycle performance of the PDCTA//K@GDY and PDCTA//bare K at 1 A g^{-1}. (c) The charge-discharge curves of the PDCTA//K@GDY and PDCTA//Bare K at 10th cycle at 1 A g^{-1}. (d) The charge-discharge curves of the PDCTA//K@GDY at 1st, 20th, 50th and 100th, at 1 A g^{-1}

odes in terms of both stability and performance. The K@GDY anode retains its capacity over 600 cycles with nearly 100% Coulombic efficiency (Fig. 4b), highlighting the excellent long-term stability and efficient ion transport facilitated by the GDY protection layer. In stark contrast, the PDCTA//bare K cells exhibit rapid capacity loss after just 10 cycles, with a dramatic decline after 200 cycles and eventual short-circuiting after 300 cycles (Fig. 4b, c).

The galvanostatic charge-discharge profiles show that the full cells with K@GDY anodes maintain a stable voltage plateau within a potential range of 1.5 to 3.5 V vs. K/K^+ at a current density of 1.0 A g^{-1}, further underscoring the superior electrochemical performance of the GDY-protected K anode (Fig. 4d). The unique triangular pore structure and high surface area of the GDY nanosheets effectively reduce local current density, prevent dendritic growth, and ensure efficient K-ion diffusion, all of which contribute to the outstanding stability and cycle life of the K@GDY anode. These results confirm that GDY-modified K metal anodes hold great potential for practical applications in potassium-ion batteries, offering enhanced cycling performance and safety. The findings emphasize the importance of using GDY as an interfacial protection layer to ensure stable plating/stripping processes, paving the way for more reliable energy storage solutions.

4 Conclusion

This work developed a microwave-assisted method for the rapid and continuous synthesis of GDY nanosheets, achieving uniform dimensions with diameters ranging from 185 to 315 nm and an average thickness of 4 nm. The microwave-enabled fast coupling reaction helps control the growth process and ensure consistency in the nanosheet morphology. The GDY nanosheets also exhibit a high specific surface area, which is key factor in their electrochemical performance. As an interfacial layer, GDY effectively inhibits the formation of K dendrites during plating and stripping processes, significantly improving the cycling stability and safety of K metal batteries. Moreover, it reduces the accumulation of dead K, enhancing the overall efficiency and prolonging the battery cycle life. This microwave-assisted synthesis approach provides a scalable and efficient means of producing high-quality GDY nanosheets, offering significant potential for use in next-generation energy storage systems.

Credit authorship contribution statement

ZHANG Jin, TONG Lian-ming and GAO Xin conceived the concept and supervised the study. KONG Ya conducted synthesis work and characterizations. ZHANG Shi-peng conducted electrochemical measurement. YIN Yu-ling and DING Feng conducted computational calculations. ZHANG Zi-xuan and FENG Xue-ting assisted with the execution of the synthesis work. KONG Ya and ZHANG Shi-peng wrote the manuscript. All the authors discussed and revised the paper.

Declaration of competing interest

The authors declare that they have no known competing financial interests or personal relationships that could have appeared to influence the work reported in this paper.

Acknowledgements

This work was financially supported by National Natural Science Foundation of China (52302034, 52402060, 52202201, 52021006), Beijing National Laboratory for Molecular Sciences (BNLMS-CXTD-202001) and Shenzhen Science and Technology Innovation Commission (KQTD20221101115627004) and China Postdoctoral Science Foundation (2024T170972).

Supporting information

Supplementary data associated with this article can be found in the online version at doi:10.1016/S1872-5805(25)60987-5.

Author information

***Corresponding author:**
TONG Lian-ming, Professor. E-mail: tonglm@pku.edu.cn;
GAO Xin, Professor. E-mail: gaoxin-cnc@pku.edu.cn
First author:
† KONG Ya and † ZHANG Shi-peng contributed equally to this work.

KONG Ya, Ph.D. E-mail: kongya_pku@163.com; ZHANG Shi-peng, Ph.D. E-mail: shipengzhang@nwpu.edu.cn

References

[1] Gao X, Liu H, Wang D, Zhang J, et al. Graphdiyne: synthesis, properties, and applications[J]. Chemical Society Reviews, 2019, 48: 908-936.

[2] Baughman R H, Eckhardt H, Kertesz M. Structure-property predictions for new planar forms of carbon: Layered phases containing sp² and sp atoms[J]. Journal of Chemical Physics, 1987, 87: 6687-6699.

[3] Chen J M, Xi J Y, Wang D, S Z, et al. Carrier mobility in graphyne should be even larger than that in graphene: A theoretical prediction[J]. Journal of Physical Chemistry Letters, 2013, 4(9): 1443-1448.

[4] Xi J Y, Wang D, Yi Y P, Shuai Z G. Electron-phonon couplings and carrier mobility in graphynes sheet calculated using the Wannier-interpolation approach[J]. Journal of Chemical Physics, 2014, 141: 034704.

[5] Long M, Tang L, Wang D, et al. Electronic structure and carrier mobility in graphdiyne sheet and nanoribbons: Theoretical predictions[J]. ACS Nano, 2011, 5(4): 2593-2600.

[6] Bu H, Zhao M, Wang A, Wang X. First-principles prediction of the transition from graphdiyne to a superlattice of carbon nanotubes and graphene nanoribbons[J]. Carbon, 2013, 65: 341-348.

[7] Narita N, Nagai S, Suzuki S, Nakao K. Optimized geometries and electronic structures of graphyne and its family[J]. Physical Review B, 1998, 58(16): 11009-11017.

[8] Luo G, Qian X, Liu H, et al. Quasiparticle energies and excitonic effects of the two-dimensional carbon allotrope graphdiyne: Theory and experiment[J]. Physical Review B, 2011, 84(7): 075439.

[9] Zheng Q, Luo G, Liu Q, et al. Structural and electronic properties of bilayer and trilayer graphdiyne[J]. Nanoscale, 2012, 4: 3990-3996.

[10] Qian X, Ning Z, Li Y, et al. Construction of graphdiyne nanowires with high-conductivity and mobility[J]. Dalton Transactions, 2012, 41: 730-733.

[11] Guo J, Shi R, Wang R, et al. Graphdiyne-polymer nanocomposite as a broadband and robust saturable absorber for ultrafast photonics[J]. Laser & Photonics Reviews, 2020, 14(4): 1900367.

[12] Srinivasu K, Ghosh S K. Graphyne and graphdiyne: Promising materials for nanoelectronics and energy storage applications[J]. Journal of Physical Chemistry C, 2012, 116(9): 5951-5956.

[13] Zheng Z, Fang H, Liu D, et al. Nonlocal response in infrared detector with semiconducting carbon nanotubes and graphdiyne[J]. Advanced Science, 2017, 4(12): 1700472.

[14] Chen Z, Molina-Jirón C, Klyatskaya S, et al. 1D and 2D graphdiynes: Recent advances on the synthesis at interfaces and potential nanotechnological applications[J]. Annalen der Physik, 2017, 529(11): 1700056.

[15] Wu P, Du P, Zhang H, Cai C. Graphdiyne as a metal-free catalyst for low-temperature CO oxidation[J]. Physical Chemistry Chemical Physics, 2014, 16(12): 5640-5648.

[16] Ren H, Shao H, Zhang L, et al. A new graphdiyne nanosheet/Pt nanoparticle-based counter electrode material with enhanced catalytic activity for dye-sensitized solar cells[J]. Advanced Energy Materials, 2015, 5(12): 1500296.

[17] Zhang H, Xia Y, Bu H, et al. Graphdiyne: A promising anode material for lithium ion batteries with high capacity and rate capability[J]. Journal of Applied Physics, 2013, 113(4): 044309.

[18] Huang C, Li Y, Wang N, et al. Progress in research into 2D graphdiyne-based materials[J]. Chemical Reviews, 2018, 118(16): 7744-7803.

[19] Xu Z, Lv X, Li J, et al. A promising anode material for sodium-ion battery with high capacity and high diffusion ability: Graphyne and graphdiyne[J]. RSC Advances, 2016, 6(30): 25594-25600.

[20] Tang H, Hessel C M, Wang J, et al. Two-dimensional carbon leading to new photoconversion processes[J]. Chemical Society Reviews, 2014, 43(13): 4281-4299.

[21] Jiao Y, Du A, Hankel M, et al. Graphdiyne: A versatile nanomaterial for electronics and hydrogen purification[J]. Chemical Communications, 2011, 47(43): 11843-11845.

[22] Cranford S W, Buehler M J. Selective hydrogen purification through graphdiyne under ambient temperature and pressure[J]. Nanoscale, 2012, 4(15): 4587-4593.

[23] Wu Y, Nian P, Liu Z, et al. Separation of acetylene, ethylene and ethane over single layered graphdiyne membranes: Performance and insights from quantum mechanical views[J]. Journal of Environmental Chemical Engineering, 2022, 10(3): 107733.

[24] Georgantzinos S K, Siampanis S G, Baldoukas A, et al. Designing the nonlinear mechanical response of graphyne structures: A finite element structural mechanics approach[J]. Materials Today Communications, 2022, 31: 103386.

[25] Mortazavi B, Shahrokhi M, Madjet M E, et al. N-, B-, P-, Al-, As-, and Ga-graphdiyne/graphyne lattices: First-principles investigation of mechanical, optical and electronic properties[J]. Journal of Materials Chemistry C, 2019, 7(10): 3025-3036.

[26] Diercks R, Armstrong J C, Boese R, et al. Hexaethynylbenzene[J]. Angewandte Chemie International Edition, 1997, 36(3): 268-269.

[27] Sakamoto J, van Heijst J, Lukin O, et al. Two-dimensional polymers: Just a dream of synthetic chemists?[J]. Angewandte Chemie International Edition, 2009, 48(6): 1030-1069.

[28] Li C L, Han Y Y, Tang S F, et al. Direct imaging and determination of the crystal structure of six-layered graphdiyne[J]. Nano Research, 2018, 11(3): 1714-1721.

[29] Gao H Y, Wagner H, Zhong D, et al. Glaser coupling at metal surfaces[J]. Angewandte Chemie International Edition, 2013, 52(14): 4024-4028.

[30] Gao X, Zhu Y H, Yi D, et al. Ultrathin graphdiyne film on graphene through solution-phase van der Waals epitaxy[J]. Science

Advances, 2018, 4(7): eaat6378.

[31] Matsuoka R, Sakamoto R, Hoshiko K, et al. Crystalline graphdiyne nanosheets produced at a gas/liquid or liquid/liquid interface[J]. Journal of the American Chemical Society, 2017, 139(8): 3145-3152.

[32] Li W H, Liu J, Yu Y X, et al. Synthesis of large-area ultrathin graphdiyne films at an air/water interface and their application in memristors[J]. Materials Chemistry Frontiers, 2020, 4(4): 1268-1273.

[33] Zeng Y, Gordiichuk P, Ichihara T, et al. Irreversible synthesis of an ultrastrong two-dimensional polymeric material[J]. Nature, 2022, 602: 91-95.

[34] Zhang G, Zeng Y, Gordiichuk P, et al. Chemical kinetic mechanisms and scaling of two-dimensional polymers via irreversible solution-phase reactions[J]. Journal of Chemical Physics, 2021, 154(19): 194901.

[35] Nishihara Y, Ikegashira K, Hirabayashi K, et al. Coupling reactions of alkynylsilanes mediated by a Cu(I) salt: Novel syntheses of conjugate diynes and disubstituted ethynes[J]. Journal of Organic Chemistry, 2000, 65(6): 1780-1787.

少层石墨双炔纳米片的微波辅助法快速、连续可控制备及其在高性能钾金属电池的应用研究

孔娅[1,2,†]，张世鹏[3,†]，殷玉玲[4,5]，张子璇[1]，冯雪廷[1]，丁峰[4,6]，
张锦[1]，童廉明[1,7,*]，高鑫[1,*]

（1. 北京大学, 化学与分子工程学院, 北京分子科学国家研究中心, 材料科学与工程学院, 北京 100871；
2. 中国航天科技集团有限公司, 中国航天科技体系与创新研究院, 北京 100088；
3. 西北工业大学, 陕西省石墨烯联合实验室, 材料科学与工程学院, 纳米能源材料中心,
凝固技术国家重点实验室, 陕西西安 710072；
4. 苏州实验室, 江苏苏州 215123；
5. 中国科学院深圳先进技术研究院, 碳中和技术研究所, 广东深圳 518055；
6. 深圳大学, 材料学院, 广东深圳 518055；
7. 北京大学深圳研究生院新材料学院, 广东深圳 518055）

摘　要： 石墨双炔（Graphdiyne，简称 GDY）作为一种新型碳同素异形体材料，具有优异的物理化学特性和广阔的应用前景。然而，实现高品质石墨双炔的高效、可控且可放量制备仍是挑战。本工作提出了一种微波辅助的单体快速偶联方法，实现了高品质石墨双炔纳米片的快速、高效且可控制备。该方法的合成速度可达 0.6 g/h，产率为 90%。制备的石墨双炔纳米片，平均直径为 246 nm，厚度为 4 nm。利用石墨双炔独特的亚纳米孔道结构和优异的物理化学性质，将其作为人工固体电解质界面（SEI）层应用于钾金属电池。测试结果表明，石墨双炔的引入显著抑制了钾枝晶的形成，并显著提升了钾金属电池的循环稳定性。进一步，利用 GDY 修饰的钾金属负极组装全电池，该电池在 600 次循环后仍表现出优异的容量保持率，库仑效率接近 100%。该工作不仅为 GDY 的合成提供了一条高效且可放量的制备途径，还为 GDY 在储能和其他前沿领域中的应用提供了新思路。

关键词： 石墨双炔；微波辅助合成；少层；钾金属电池；无枝晶生长

中图分类号： TQ152　　　**文献标识码：** A

基金项目： 国家自然科学基金（52302034, 52402060, 52202201, 52021006）；北京分子科学国家研究中心（BNLMS-CXTD-202001）；深圳市科技创新委员会（KQTD20221101115627004）；中国博士后科学基金（2024T170972）

通讯作者： 童廉明, 研究员. E-mail: tonglm@pku.edu.cn；
高鑫, 研究员. E-mail: gaoxin-cnc@pku.edu.cn

第一作者： †孔娅和†张世鹏为共同第一作者.
孔娅, 博士. E-mail: kongya_pku@163.com；
张世鹏, 博士. E-mail: shipengzhang@nwpu.edu.cn

本文的电子版全文由 Elsevier 出版社在 ScienceDirect 上出版（https://www.sciencedirect.com/journal/new-carbon-materials/）